ITTC Quality System Manual

Recommended Procedures and Guidelines

Procedure

Uncertainty Analysis, Laser Doppler Velocimetry Calibration

7.5 Process Control

7.5-01 Test Preparation

7.5-01-03 Instrumentation, Calibration

7.5-01-03-02 Uncertainty Analysis, Laser Doppler Velocimetry Calibration

Updated / Edited by	Approved
Quality Systems Group of 28th ITTC	25th ITTC 2008
Date 09/2016	Date 09/2008

Table of Contents

Uncertainty Analysis: Laser Doppler Velocimetry (LDV) Calibration

1. PURPOSE OF PROCEDURE

The purpose of this procedure is to describe methods for the calibration of a laser Doppler velocimetry (LDV), which is also known as a laser Doppler anemometer (LDA). The procedure also provides methods for evaluation of the uncertainty in the calibration.

2. SCOPE

The description in this procedure is limited to the velocity calibration of an LDV system and its uncertainty. A typical commercial LDV system is dual beam and consists of a fibre-optic probe, signal processors, traversing system, processing software, and argon-ion laser. The systems are usually two velocity components with a single fibre-optic probe. A third component is possible with a second single component probe. Details of the operation and alignment of a commercial system are described in the manufacturer's manual. A number of references are available on the principles of LDV systems. Three examples are Adrian (1996), Buchhave, et al. (1979), and Durst, et al. (1976). ITTC Procedure 7.5-02-03-02.3 is an LDV guide for propulsor applications. The current procedure assumes a fundamental knowledge of an LDV and is independent of the type of application.

3. GENERAL

The fundamental equation of an LDV is given from Adrian (1996) by

$$V = \delta_f f_D \tag{1}$$

where δ_f is the fringe spacing in μm and f_D is the Doppler frequency in MHz. The fringe spacing is also the velocity calibration factor in m/s/MHz. The Doppler frequency is measured by the signal processor while the fringe spacing is determined by the optics

$$\delta_f = \lambda / (2 \sin \kappa) \tag{2}$$

where λ is the wavelength of the laser and κ is the half-angle of the beam intersection angle. The half-angle is then related to f, the focal length of the lens, and D, the spacing between the exit beams by

$$\kappa = A\tan[D / (2 f)] \tag{3}$$

From these optical parameters, the dimensions of the probe volume may also be calculated. These may be important for the determination of the spatial resolution of the optical probe and calculation of the required seed particle concentration. The probe volume is ellipsoidal in shape. The beam waist diameter at the focal point for a Gaussian beam is given by

$$d_e = 4 f\lambda / (\pi M d) \tag{4}$$

where M is the magnification factor for a beam expander and d is the input beam diameter. The input beam diameter is defined by the fibre diameter of the transmitting fibre. For a standard optical system, the beam diameter is defined by the laser. As equation (4) indicates, the beam waist diameter is decreased by the magnification of the beam expander. The diameter and length of the probe volume are then

$$d_m = d_e / \cos\kappa \tag{5}$$

$$l_m = d_e / \sin\kappa \tag{6}$$

The number of fringes is

$$N_{\mathrm{f}} = d_{\mathrm{m}} / \delta_{\mathrm{f}} \qquad (7)$$

From equation (6), a lens with a long focal length and small beam spacing results in a long probe volume. The volume enclosed by the ellipsoid is

$$V_{\mathrm{m}} = \pi d_{\mathrm{e}}^{3} / (6 \cos\kappa \sin\kappa) \qquad (8)$$

An example calculation of the probe volume characteristics in air is shown in Table 1.

Parameter	Symbol	Units	Value	Value
Beam dia.	d	mm	1.35	1.35
Beam expan.	M		2.775	2.775
Beam space	D	mm	115	115
Focal length	f	mm	1600	1600
Wave length	λ	nm	488.0	514.5
Half angle	κ	deg	2.03	2.03
Fringe space	δ_{f}	µm	6.89	7.28
Beam waist	d_{e}	µm	265	280
Probe dia.	d_{m}	µm	266	280
Probe length	l_{m}	mm	7.49	7.91
No. fringes	N_{f}		38	38

Table 1: Example LDV probe volume in air

The data in Table 1 is from Park, et al. (2002). For this probe orientation, the blue beams (488.0 nm) were the vertical velocity component, while the green beams (514.5 nm) were the axial velocity component. The probe length in water will increase by a factor of 4/3, the index of refraction of water from IAPWS (1997). The fringe spacing or velocity calibration factor and the probe diameter will be the same in water as in air. For the probe lengths in the table, the lengths in water will be, respectively for the blue and green beams, 10.0 and 10.5 mm. Likewise the probe volume in equation (8) will increase by a factor of 4/3 in water.

4. CALIBRATION

4.1 Calibration of optics.

For commercial LDV systems, processor information is converted to velocity through software with equation (1). From equation (1), the combined uncertainty in velocity is then given from the uncertainty equation by

$$u_V = \sqrt{[f_{\mathrm{D}}(\partial\delta_{\mathrm{f}} / \partial\kappa) u_\kappa]^2 + [\delta_{\mathrm{f}} u_{f_{\mathrm{D}}}]^2} \qquad (9)$$

where the uncertainty in the wavelength of the laser is negligible. For modern signal processors, the uncertainty in the measurement of the Doppler frequency can be assumed negligible. The uncertainty is then determined by an accurate measurement of the beam intersection half-angle, κ, where the beam intersection angle is computed from equation (3). The uncertainty in κ is then determined by the uncertainty in the measurement of the beam spacing and focal length.

Bean and Hall (1999) have described a precise method for the measurement κ. The position of a transmitted laser beam was detected by a photo-diode mounted behind a 0.25 mm vertical slit. The photo-diode was mounted on a translation stage that was traversed normal to the axis of the fibre-optic probe. The fibre-optic probe was mounted on a translation stage that traversed in a direction along the axis of the probe. For a fixed position, the distance between the axis of the laser and the location of the laser beam was measured as the distance CE. The laser was then translated toward the laser-diode translation stage by the distance AB, and the distance between the new positions of the laser beam was measured as the distance CD. The half-angle was then computed as

$$\kappa = 2A\tan[(CE - CD)/AB] \quad (10)$$

In the Bean and Hall (1999) example, the distance *AC* was 2.9 m, and the length *CE* was 0.86 m. Additional details are described in Bean and Hall (1999). By this method, their uncertainty in velocity was ±6 mm/s.

4.2 Calibration by spinning disk

4.2.1 Theory

The preferred method for calibration of an LDV is by the spinning disk method. A spinning disk is a primary standard for velocity. In this case, the LDV is calibrated directly in velocity units. Since LDV processors are highly accurate, the method is essentially an indirect method for measurement of the beam intersection angle. The velocity from a spinning disk is

$$V = r\omega = 2\pi f_{\mathrm{r}} r \quad (11)$$

where r is the disk radius, ω is the rotational speed in radians/s, and f_{r} is the rotational frequency in Hz (revolutions/s). The combined uncertainty in the velocity is then

$$u_V = \sqrt{(2\pi r u_{f_{\mathrm{r}}})^2 + (2\pi f_{\mathrm{r}} u_r)^2} \quad (12)$$

From calibration theory, the velocity from LDV as measured by the rotating disk as the reference velocity is given by linear regression analysis for a range of velocities

$$V_{\mathrm{LDV}} = a + bV \quad (13)$$

Nominally, a = 0 and b = 1. If the optical parameters were precisely known, these values would be precisely 0 and 1 within the statistical uncertainty of the curve fit.

The combined uncertainty in an LDV measurement then has 3 elements in the uncertainty.

- Uncertainty in the reference velocity of the spinning disk from equation (12).
- Uncertainty from the prediction limit of equation (13).
- Uncertainty by the Type A method from the time series associated with the average value of the velocity as measured by the LDV.

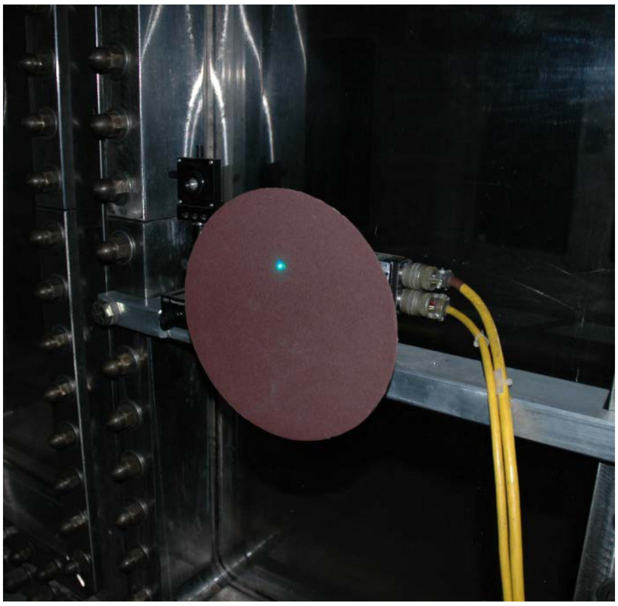

Figure 1: Photograph of rotating disk

4.2.2 Example

As an example from Park, et al. (2002), the LDV was calibrated with a rotating sandpaper disk shown in Figure 1. For reference, the diameter of the disk is 229 mm (9 inches) in diameter with a precision-drilled hole at the centre of the disk with a diameter of 1.02 mm (0.040 inch). The surface of the disk is covered with 60-grit emery paper. The motor is digitally controlled by computer. The motor turns both clockwise and counter-clockwise and has an optical encoder with a resolution of 2,000 steps per revolution. The manufacturer's specification on the expanded uncertainty of the motor speed is ±0.04 rps (revolutions/s or Hz). The focal point of the laser is located 50 mm above the centre in Figure 1. The resolution of the digitally controlled traversing system is 5 µm.

An advantage of the rotating disk is that a 2-component LDV can be calibrated on the disk. Figure 1 shows the location on the disk above the centre for calibration of the axial velocity component. The vertical component is calibrated either to the left or right of the centre. When the laser probe is properly located, the vertical velocity component should be zero during calibration of the axial component and visa versa.

The uncertainty in the velocity from the rotating disk is presented in Figure 2 for a radial location of 100 mm. As the figure indicates, the dominant uncertainty term is from the uncertainty in the rotational speed of ±0.04 rps with a nearly constant value of ±0.025 m/s. The uncertainty in the radius was from 6 repeat locations of the centre of the disk. With the Student *t* from ISO (1995) as the coverage factor, the uncertainty in the location of the centre of the disk was ±0.031 mm. At the maximum speed of 18 m/s, the estimated expanded uncertainty is ±0.026 m/s (0.14 %) at the 95 % confidence limit.

From equation (12), both the radius and the uncertainty in the in the rotational rate are fixed, the uncertainty in velocity could be reduced by a factor nearly 2. The result for a 50 mm radius is shown in Figure 3. Other factors become relatively more important, but a significant reduction in the combined uncertainty is evident. The estimated expanded uncertainty at 18 m/s is now ±0.017 m/s (0.094 %).

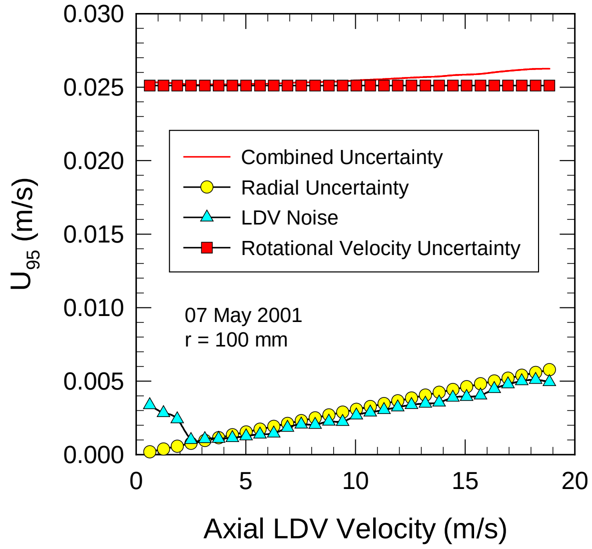

a. Absolute uncertainty

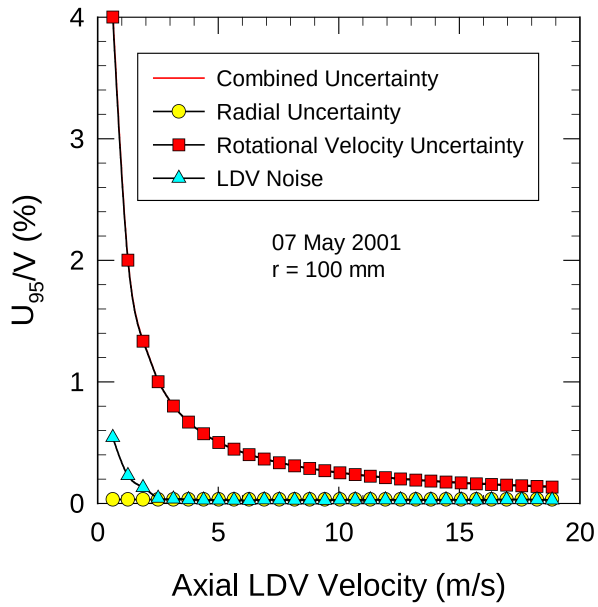

b. Relative uncertainty

Figure 2: Velocity uncertainty of rotating disk for *r* = 100 mm

As Figure 2 and Figure 3 indicate, the contribution to the combined uncertainty from the LDV noise is relatively small. For a typical LDV, the noise as relative standard uncertainty or relative turbulence intensity is less than 1 % and is nearly constant independent of velocity.

In this particular example, the LDV noise was an average of 0.42 % for velocities greater than 4 m/s. For 1000 samples and a coverage factor of 2, the Type A uncertainty is ±0.026 %.

Other possible contributions to the uncertainty include alignment of the fibre-optic probe. Such misalignment was assumed to be small. The traversing system and fibre-optic probe were levelled with a precision electronic level.

For the example calibration, the LDV was calibrated in 1 rps increments from 1 to 30 rps. The results are shown in Figure 4. Slope and intercept corrections were obtained by linear regression analysis as described in the ITTC Procedure 7.5-01-03-01 (2008).

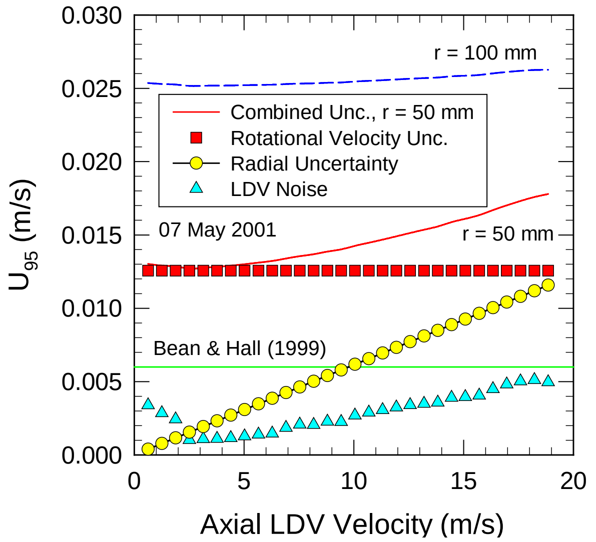

Figure 3: Absolute velocity uncertainty of rotating disk with r = 50 mm

As Figure 4a indicates, all of the data points lie on a straight line, and the uncertainty in the measurement is smaller than the symbols. The variation of the data relative to the curve fit is shown in Figure 4b. In this format, the uncertainty in the individual measurements as indicated by the error bars is also readily evident. The plot also indicates 2 outliers that were not excluded from the regression analysis. The 2 outliers were not excluded for 3 reasons: (1) the slope and intercept were not appreciably altered, (2) the reduction in the uncertainty from the curve fit was not reduced appreciably, and (3) the uncertainty in the individual measurements as indicated by the error bars was large in comparison to the data scatter.

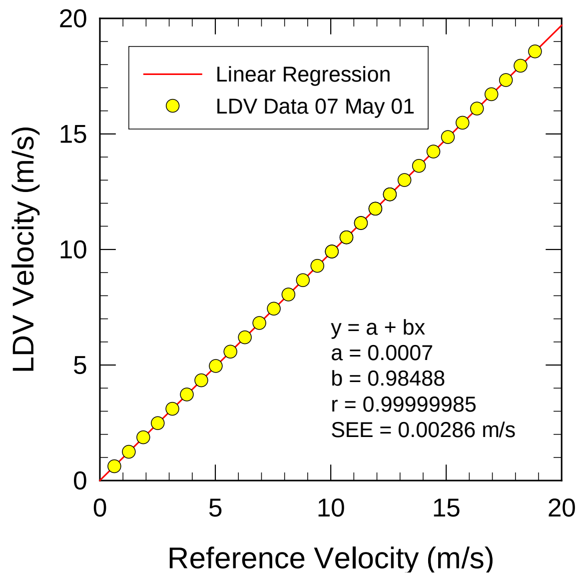

a. Linear plot

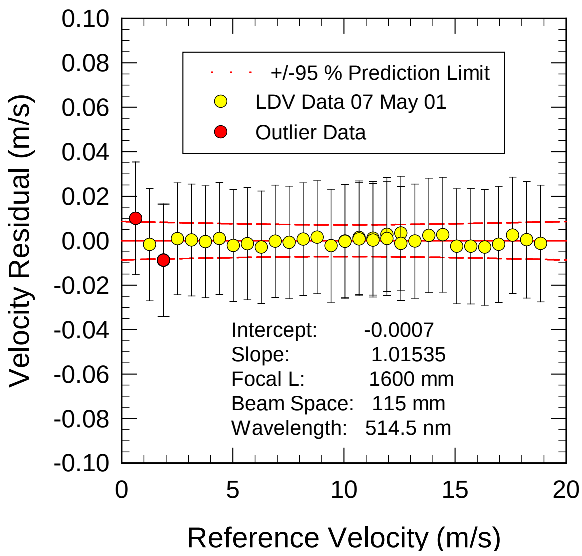

b. Residual plot

Figure 4: LDV calibration by rotating disk

The dashed line in Figure 4 is the uncertainty from the prediction limit from calibration theory as described in the ITTC Procedure 7.5-01-03-01 (2008). In this particular case, the uncertainty from the prediction limit at 18 m/s was ±8.2 mm/s (0.046 %) in comparison to ±26 mm/s (0.14 %) from the uncertainty in velocity from the rotating disk at a radial location of 100 mm. With the 2 outliers excluded, the prediction limit at 18 m/s becomes ±5.1 mm/s (0.028 %).

The slope and intercept correction is listed in Figure 4b as 1.01535 and –0.0007, respectively. A hypothesis test may be applied to determine whether these corrections are statistically different from 1 and 0. The *t*-value for the slope is 159, while the *t*-value for the intercept is 0.63. Clearly at the 95 % confidence limit, the slope fails a hypothesis test, but the intercept passes.

4.3 Other spinning disk methods

4.3.1 Spinning wire

Another method is the spinning wire, which has been applied at 2 NMIs (National Metrology Institute): the National Institute of Standards and Technology (NIST) in the USA by Bean and Hall (1999) and Yeh and Hall (2007) and the National Metrology Institute of Japan (NMIJ) by Kurihara, et al. (2002). The spinning wire method from Yeh and Hall (2007) is shown schematically in Figure 5. In both laboratories the wire was a 5 μm diameter tungsten wire. The diameter of the cylinder is measured to very high precision with a laser coordinate measurement system. For the NIST system, the diameter was measured as 136.522 mm with an uncertainty of 10 μm. The resulting uncertainty in speed is ±0.0073 %. By comparison, NMIJ claims an uncertainty of 0.0019 % in velocity from a nominal diameter of 200 mm at 20 m/s.

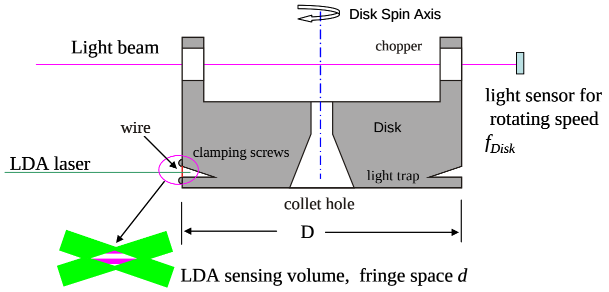

Figure 5: Spinning wire schematic at NIST by Yeh and Hall (2007)

A significant difference of the spinning wire is that only a single particle passes through the probe volume per revolution in comparison to multiple particles for sandpaper disk. One unique feature is the measurement of the divergence of the fringes. The effect on fringe spacing is measured by translation of the fibre-optic probe along the length of the probe volume. Yeh and Hall (2007) measured the expanded uncertainty of this effect as ±0.16 %.

At NIST, the 3 main contributors to the uncertainty in velocity from the spinning wire calibration were the rotational speed, fringe divergence, and LDV processor. The uncertainties in velocity were respectively 0.26, 0.36, and 0.16 % for a combined and expanded uncertainty of ±0.47 %.

At NMIJ, they discovered that the wire deflected at high speed but developed an accurate method of calibration of the diameter for the compensation of the wire deflection. The typical uncertainty in velocity in the rotating disk itself was ±0.018 %. However, the uncertainty was dominated by the performance of the LDV processor. At NMIJ, the velocity uncertainty was estimated to be ±0.2 %.

4.3.2 Glass disk

Another primary velocity standard is a precision rotating glass disk by Lu, et al. (2001) at

Physikalish-Technische Bundesanstalt (PTB) in Germany. In this case, velocity is measured on the cylindrical surface normal to the axis of rotation rather than on the flat surface for the sandpaper disk. Similarly to the sandpaper disk, the rotating glass disk also senses multiple particles per revolution. The static radius was measured with an expanded uncertainty of ±0.014 %. However, the radius was also measured dynamically with a standard deviation of 0.0187 mm, where the mean radius was 92.1 mm. The relative expanded uncertainty in velocity from the radius was then ±0.020 %.

The next largest uncertainty was in the rotational rate with a value of ±0.018 %. The combined and expanded uncertainty was estimated to be ±0.055 %. Their estimate also included the uncertainties in the Doppler frequency and angular alignment of the laser and disk, which were smaller at 3.6 % of the combined uncertainty.

4.3.3 Disk design considerations

The previously described disks can be the basis for an accurate primary velocity standard for an LDV. The essential features are a disk with accurately measured dimensions and a digitally controlled motor with a high-resolution optical encoder. During a calibration, the rotational speed may be measured from the pulse output of the optical encoder with an accurate frequency counter or data acquisition card (DAC) with a counter port. The DAC should have certified timing.

The rotational speed is then from the ITTC Procedure 7.5-01-03-01 (2008):

$$f_r = n/(pt) \tag{12}$$

where n is the number of pulses, p is the number of pulses per revolution, and t is the time. The uncertainty in the time is from the calibration certificate for the DAC. The standard uncertainty in n for a uniform probability density function is

$$u_n = a/\sqrt{3} \tag{13}$$

where a = ±½ pulse. For a motor with an optical encoder of 1000 steps, the standard uncertainty in the number of pulses is ±0.029 % per revolution or ±0.0029 % in 10 revolutions. The combined uncertainty for the rotational frequency from the ITTC Procedure 7.5-01-03-01 (2008) is

$$(u_{f_r}/f_r)^2 = (u_n/n)^2 + (u_t/t)^2 \tag{14}$$

With information in this procedure, the uncertainty in velocity of a particular design may be estimated before parts are purchased or manufactured. With a properly designed system, the uncertainty in velocity for an LDV should be easily between ±0.1 and ±0.2 %.

An advantage of the rotating sandpaper disk is that a 2-component probe can be easily calibrated by traversing the laser to the appropriate point on the disk. Different values of the radius are also possible. For the rotating wire or glass disk, the fixture would have to be rotated 90° for the vertical velocity component, and the radius is fixed.

A potential advantage of the rotating wire design is that it could be applied in the calibration of a 3-component velocity system. Figure 5 shows the calibration configuration for the axial component of velocity. By translation of the fibre-optic probe, the on-axis component could be measured. Rotation of the disk 90° would allow calibration of the vertical and on-axis components.

Element	NSWC	NIST	NMIJ	PTB
r	0.061	0.0074	0.0017	0.041
f_r	0.062	0.26	0.0018	0.035
δ_f	---	0.16	---	---
Angle	---	0.011	0.017	0.0022
f_D	0.026	0.36	0.20	0.010
Curve fit	0.043	---	---	---
Combined	0.10	0.48	0.20	0.055

Table 2: Comparison of expanded uncertainty estimates in % at 20 m/s

A comparison of the uncertainty estimates for the laboratories previously discussed are summarized in Table 2. In this table, δ_{fr} at NIST refers to the uncertainty in velocity from the divergence of the fringes. Angle refers to the various alignments in angle in the LDV calibration such as inclination of the LDV probe or inclination of the rotating disk relative to the probe. In the NSWCCD case, angle uncertainty was not considered important, which is confirmed by the other 3 laboratories. The f_D is the Type A uncertainty in velocity as measured by the processors. Only NSWCCD has included an uncertainty in the curve fit from a range of velocity calibrations. Such uncertainty should be considered since slope and intercept will be applied in the correction of measured data. The NSWCCD estimates are from a 50 mm radius.

5. OPERATIONAL PROCEDURES

5.1 Optical alignment

For optical alignment of the LDV, the manufacturer’s manuals should be consulted, but some general guidelines are provided here.

5.1.1 Adjustment of light power

First, the output of the each pair of beams should be adjusted so that they are nearly the same. Perform the following steps.

- Locate a laser light meter at an output beam of the fibre-optic probe and adjust the laser power to a setting typical of normal measurements.
- Adjust the fibre manipulators so that a maximum value is read on the light meter and record the meter reading.
- Move the light meter to the second beam, measure, and record the reading.
- Adjust the Bragg cell so that the light meter reads the average of the 2 readings.
- Move the light meter to the first beam, measure, and record the meter reading.
- If the 2 readings are reasonably close, this adjustment is complete. If not, repeat the procedure.
- If the probe has 2 components, repeat this process for the other pair of beams. Since a 2-component system typically has one Bragg cell, matching the intensity will be a compromise between two pairs of beams.

5.1.2 Beam crossing adjustment

Beam crossing should be checked. For some probes, a factory adjustment is required. Beam crossing point may be checked with either a 30X microscope objective or a precision pinhole with a diameter of about half the estimated probe diameter. The microscope objective or pinhole should be mounted on a precision XYZ optical translation stage with a sensitivity of 1 μm (one micron).

For these alignment procedures, the laser should be operated near minimum power. Laser goggles should be worn when viewing the focal point.

First, the focal point of the fibre-optic probe should be located. Turn off the photo-multiplier tubes. Illuminate the end of the receiving fibre with a laser beam at low power while the normally transmitted beams are blocked. Then, locate the focal point. This will insure that the scatter light is focused on the receiving fibre. For the microscope objective, the focal is located when the spot on the opposite wall is the smallest. For the pinhole, the illuminated spot will be the largest.

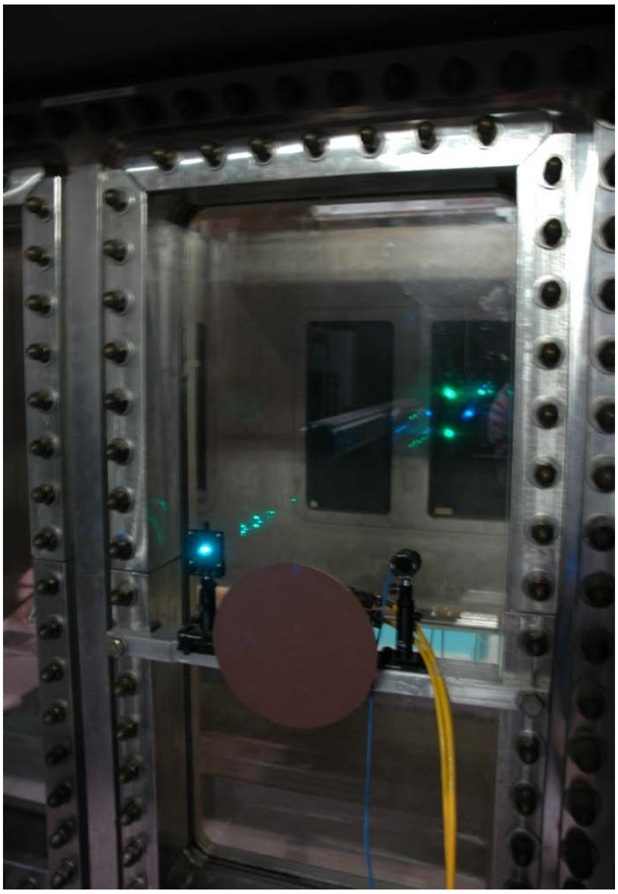

Figure 6: Photograph of a focused 4-beam probe

Unblock the transmitted beams. Adjust the beams so that they are focused on the focal point as determined by the receiving fibre. For the microscope objective, all beams should merge as single point on the opposite wall. A darkened room may be necessary to see the beams.

If a pinhole is used, the pairs of beams should be illuminated on the opposite wall. When properly focused, the beam pairs should be circular and have the same intensity to the eye. For a properly functioning laser with a Gaussian distribution of light intensity, the light intensity at the beam centre should appear the brightest. The result of the 4-beam probe is shown in Figure 6.

5.2 Calibration procedure

For calibration of the LDV by spinning disk, locate the probe volume at the measurement point and perform the following steps:

- First, set the laser power at a relatively low value and reduce the PMT voltage to on the order of 500 V.
- Accurately locate the centre of the disk. In the sandpaper disk example, a reference hole was located at the centre of the disk. A better alternative may be to locate the centre of the disk on the basis of the measurement of the disk diameter. The centre may be located as the average of the measurement of the horizontal location of the edge of the disk at the left and right, while the disk is rotating. The vertical location is established as the average of the measurements of the top and bottom. The traversing system may then be re-indexed with these values so that the disk centre is zero.
- Locate the probe volume at a point relative to the measurement point so that the data rate is a maximum. Nominally, the maximum data rate will occur at the mid-point of the probe volume length, $l_m/2$. Translation normal to the disk is required for determination of the maximum data rate. Location of the optimum can be facilitated by documentation of the data rate as a function of position.
- Adjust the PMT voltage for a reasonable data rate at low speed for a data rate on the

order of 1 kHz or less on the LDV processor. Of course, the data rate will increase as the disk speed increases.

- If the probe is a two-component probe, rotate the head until the orthogonal component is zero at all rotational speeds. After adjustment for zero velocity, the above steps may need to be repeated.
- For a two-component probe and coincident velocity measurements, the data rate for both components should be a maximum at the same location. If not, the beams should be re-adjusted. This can be done on the rotating disk by adjustment of the laser beams so that the data rate is a maximum at the same point.
- Calibrate the probe over the required velocity range with at least 10 equal velocity increments per the ITTC Procedure 7.5-01-03-01 (2008) and compute the correction slope and intercept by linear regression analysis.
- The number of samples collected for each velocity should be on the order of several revolutions of the disk. Two measurements are recommended so that the disk speed is verified as stable.
- The mean value and standard deviation at each point should be computed from about 1000 samples. The Type A uncertainty may then be computed from this data.
- An evaluation of fringe divergence is recommended. Velocity calibration should be repeated at probe locations on the order of $l_m/4$ (one-quarter of the probe length) from equation (6) on both sides of the measurement location ($l_m/2$) at the maximum data rate. That is, velocity calibration is recommended at $l_m/4$, $l_m/2$, and $3l_m/4$.

Finally, the data in post-processing may be corrected with the slope and offset acquired during calibration. However, this data may also be entered in the LDV processor software. From equation (2), a corrected beam intersection angle may be computed as

$$\kappa_2 = A\,sin(b\,sin\,\kappa_1) \tag{14}$$

and a corrected beam spacing from equation (3) with the focal length, *f*, fixed at the specification for the transmitting lens is

$$D_2 = 2f\,\tan\kappa_2 \tag{15}$$

where the subscripts 1 and 2 are for the old and new values, respectively, and *b* is the slope from the linear regression analysis. With these corrections, the processors will produce a calibrated velocity directly. The corrected values should be checked with the spinning disk method previously outlined.

The repeated calibration should provide a slope and intercept of 1 and 0, respectively. Statistically, the results for slope and intercept may be checked by a hypothesis test.

6. SUMMARY

With the application of the methodology outlined here, a rotating disk will be a primary standard in velocity with an expanded uncertainty on the order of ±0.1 to ±0.2 %. The main factors for low uncertainty are a disk with an accurately measured radius and a precision digitally controlled motor. With modern technology, a very precise radius with known uncertainty can be measured with a laser based coordinate measurement device. The digitally controlled motor should have an optical encoder with at least 1000 steps per revolution. The traversing system for location of the probe volume should have a resolution of 5 μm in comparison of a typical probe volume with a diameter of 200 μm. The speed of the disk may be controlled through computer software, and the LDV data are acquired through software. Consequently, an LDV may be calibrated in a relatively short period of time with low uncertainty.

These procedures do not include possible distortion when the measurements are obtained through a window. If possible, the window should be fabricated from optical glass.

7. LIST OF SYMBOLS

D	Laser beam spacing	m
d	Laser beam input diameter	m
d_e	Gaussian beam waist diameter	m
d_m	Measurement volume diameter	m
f	Lens focal length	m
f_D	Doppler shift frequency	Hz
f_r	Rotational rate	Hz
l_m	Measurement volume length	m
M	Beam expander magnification factor	1
N_f	Number of fringes	1
n	Number of pulses	1
p	Number of pulses per revolution	1
r	Radius	m
t	Time	s
U	Expanded uncertainty	
u_x	Standard uncertainty of measurement variable, x	
V	Velocity	m/s
V_m	Ellipsoidal measurement volume	m^3
δ_f	Fringe Spacing	m
κ	Beam intersection half angle	°
λ	Laser wavelength	m
ω	Rotational rate, $2\pi f_r$	rad/s

8. REFERENCES

Adrian, R. J., 1996, "Chapter Four: Laser Velocimetry", Fluid Mechanics Measurements, Second Edition, edited by Richard J. Goldstein, Washington: Taylor and Francis, pp. 175-299.

Bean, V. E. and Hall, J. M., 1999, "New Primary Standards for Air Speed Measurement at NIST", Proceedings of 1999 NCSL Workshop and Symposium, Charlotte, North Carolina USA, pp. 413-421.

Buchhave, P., George, W. K., and Lumley, J. L., 1979, "The Measurement of Turbulence with the Laser-Doppler Anemometer", Annual Review of Fluid Mechanics, Vol. 11, pp. 443-503.

Durst, F., Melling, A., and Whitelaw, J. H., 1976, Principles and Practice of Laser Doppler Anemometry, New York: Academic Press.

IAPWS, 1997, "Release on the Refractive Index of Ordinary Water Substance as a Function of Wavelength, Temperature and Pressure", The International Association for the Properties of Water and Steam," Erlangen, Germany.

ISO, 1995, "Guide to the Expression of Uncertainty in Measurement", International Organization for Standardization, Genève, Switzerland.

ITTC, 1999, "Testing and Extrapolation Methods Propulsion, Propulsor Guide for Use of LDV", ITTC Procedure 7.5-02-03-02.3.

ITTC, 2008, "Uncertainty Analysis: Instrument Calibration", ITTC Procedure 7.5-01-03-01.

Lu, J., Mickan, B., Shu, W., Kurihara, N., and Dopheide, D., 2001, "Research of the LDA

Calibration Facility's Uncertainty", Physikalisch-Technische Bundesanstalt (PTB), Germany.

Kurihara, N., Terao, Y., and Takamoto, M., 2002, "LDV Calibrator for the Air Speed Standard Between 1.3 to 40 m/s", Paper No. 61, 5th International Symposium on Fluid Flow Measurement, Arlington, Virginia USA.

Park, J. T., Cutbirth, J. M., and Brewer, W. H., 2002, "Hydrodynamic Performance of the Large Cavitation Channel (LCC)", Technical Report NSWCCD-50-TR—2002/068, Naval Surface Warfare Center Carderock Division, West Bethesda, Maryland USA.

Yeh, T. T., and Hall, J. M., 2007, "An Uncertainty Analysis of the NIST Airspeed Standards", ASME Paper FEDSM2007-37560, 5th Joint ASME/JSME Fluids Engineering Conference, San Diego, California USA.